nature energy

ARTICLES

https://doi.org/10.1038/s41560-018-0290-1

Combined economic and technological evaluation of battery energy storage for grid applications

D. M. Davies[1], M. G. Verde[1], O. Mnyshenko[2], Y. R. Chen[2], R. Rajeev[1], Y. S. Meng[1,3*] and G. Elliott[2,3*]

Batteries will play critical roles in modernizing energy grids, as they will allow a greater penetration of renewable energy and perform applications that better match supply with demand. Applying storage technology is a business decision that requires potential revenues to be accurately estimated to determine the economic viability, which requires models that consider market rules and prices, along with battery and application-specific constraints. Here we use models of storage connected to the California energy grid and show how the application-governed duty cycles (power profiles) of different applications affect different battery chemistries. We reveal critical trade-offs between battery chemistries and the applicability of energy content in the battery and show that accurate revenue measurement can only be achieved if a realistic battery operation in each application is considered. The findings in this work could call for a paradigm shift in how the true economic values of energy storage devices could be assessed.

Energy storage systems (ESSs) play critical roles in the successful operation of energy grids by better matching the energy supply with demand and providing services that help grids function. The use of ESSs requires that they are economically viable for the owner of the system. Batteries have drawn much attention for grid-scale storage due to their scalability and ability to perform a variety of functions. Grid-connected batteries provide a wide range of potential revenue depending on the application. Eyer and Corey[1] summarize the opportunities for batteries to participate in applications such as arbitrage, congestion relief, renewable integration and grid ancillary services. By participating in these applications, batteries help to maintain and improve the performance of the grid and also potentially provide a source of revenue to the owner. For an economically feasible implementation, accurate estimates of revenues are required across battery technologies and applications of the battery to assess the financial potential of the device. From the perspective of modelling revenues, constructing accurate estimates of revenues requires models that take into account the rules of operation, realistic market prices for services and the energy and power constraints of the storage device.

Previous estimates of revenue vary greatly, based on the particular market, storage technology and the assumptions of the operation of the storage technology[2–5]. For example, a summary by Fitzgerald et al. estimates revenues for load shifting that equate to the operation of a 1 MWh battery from near US$0 to US$274 per day[6]. Such large variations can be attributed to uncertainties in the operating conditions. Additionally, the literature often overlooks the interaction of the storage technology with the application itself, assuming a similar performance of a technology across different applications. This problem is seen in the evaluation of battery technologies, in which typical battery testing uses a constant current mode with the electrochemical voltage change tracked as a function of time.

A more precise understanding of potential revenues and ESS valuation is obtained by making modelling choices as close to real-world applications as possible and by testing batteries on schedules that mimic these applications. This includes following the rules of particular markets as closely as possible, choosing schedules for the operation of the storage device using forecasts rather than known energy prices. Testing batteries using varying dispatches and rates of power dictated by the application will probably lead to values of coulombic efficiency, voltaic efficiency and total energy efficiency that are different from the values obtained from traditional testing methods, such as the constant current mode.

Sandia National Laboratories separates the revenue-generating grid applications into five categories, with one category devoted to utility customers[1]. By choosing applications that are included in the remaining four categories (electric supply, ancillary services, grid system applications and renewable integration), we are able to gain a broad understanding of the revenue generation and storage performance across the whole system. The applications we examine here are: time shift in the day-ahead market (DAM) (Fig. 1a), congestion relief (Fig. 1c), flexible ramping (Fig. 1d) and frequency regulation (Fig. 1e). The energy-shifting timescales of all these applications are relatively short, with the longest discharge or charge for all the applications spanning a maximum of three hours. Using data from the California market, we evaluated five different battery chemistries. Our calculations use market prices where available from the California Independent System Operator (CAISO) market and are computed over a period of two years of virtual operation of the device. Each revenue calculation produces a duty cycle (power profile, as defined by Sandia National Laboratories[7]) for the batteries, which is used to test the performance of the batteries.

We evaluated revenues with a model of the storage device and show that both revenue and the best application of any ESS are highly dependent on the cell-level battery efficiency of the ESS. We established a technique to measure the efficiency of the batteries that perform these application-based duty cycles and show that battery efficiency, in turn, depends on how the battery is utilized to generate the revenues. As the revenue of each application is dependent on the efficiency of the battery, this results in non-obvious optimal battery/application pairings for revenue generation. This study integrates both the economic evaluation of storage with parameters generated

[1]Department of NanoEngineering, University of California San Diego, La Jolla, CA, USA. [2]Department of Economics, University of California San Diego, La Jolla, CA, USA. [3]Sustainable Power and Energy Center (SPEC), University of California San Diego, La Jolla, CA, USA. *e-mail: shmeng@ucsd.edu; grelliott@ucsd.edu

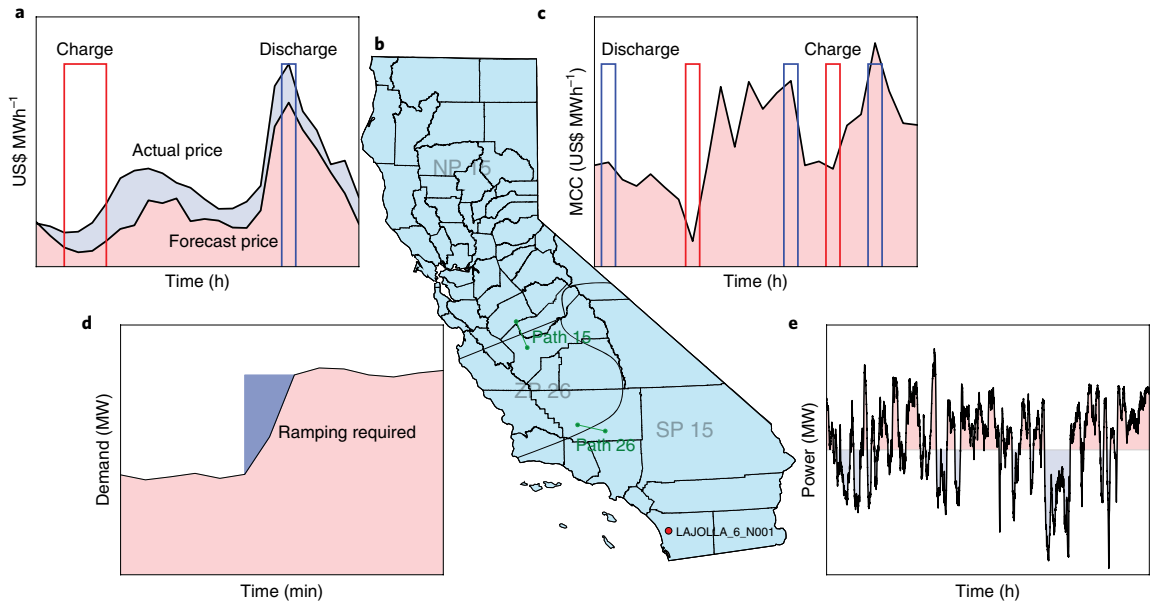

Fig. 1 | California electricity transmission paths and the four applications examined. The central image (**b**) shows where the data were obtained. The red dot shows the primary node (LAJOLLA_6), from which the pricing and power data used in this article were obtained for the application duty cycles. The green paths show the location of California's two major transmission paths and the corresponding ancillary service regions NP15 (north of Path 15), SP15 (south of Path 15) and ZP26 (south of Path 15 and north of Path 26). **a**,**c**–**e**, The graphs depict the four different application duty cycles considered here: energy time shift (**a**), congestion relief (**c**), flexible ramping (**d**) and frequency regulation (**e**).

from testing the batteries under the scenario used to construct the revenues and demonstrates the importance of an application-based battery evaluation to grid-scale revenue prediction.

Battery model

Grid-connected batteries in the form of ESSs are often complicated and contain power electronics and maintenance systems. The interaction of these systems with different battery chemistries themselves is complicated. For example, the performance of lithium ion batteries is often more temperature dependent than that of lead–acid (PbA) batteries[8], and so the chemistries may require different thermal management systems. This complication is further enhanced by the interaction of the power electronics with application duty cycles. Inverters, for example, are designed for a certain power output and operate less efficiently at other powers[9]. Therefore, an inverter would probably perform at a lower efficiency during the frequency-regulation application (which has many power fluctuations) than the time-shift application. Rather than guessing at the efficiencies of the power electronics and maintenance systems, we excluded their effects from this article. The present study focuses on the performances of the fundamental building blocks (cell-level batteries) of these storage systems for a variety of applications and future work will take the effects of additional variables, such as power electronics, into account.

The storage device is modelled by a discretized equation that governs the state of energy (Fig. 2). The state of energy S_t^{E} at time t follows the process:

$$S_t^{\mathrm{E}} = S_{t-1}^{\mathrm{E}}\gamma_{\mathrm{SD}} + \gamma_{\mathrm{PE}}P_t^{\mathrm{C}_t} - \gamma_{\mathrm{B}}^{-1}P_t^{\mathrm{D}}t \quad (1)$$

where S_{t-1}^{E} is the state of energy at the end of the previous time step, and the maximum available energy (S^{E}) is measured in megawatt hours. The time step t is either 15 minutes (in the real-time market; RTM) or one hour (in the DAM) depending on the application. P_t^{C} and P_t^{D} are the average charge and discharge rates (the rate of power (measured in megawatts) that the grid either gives to or receives from the ESS), respectively, during timestep t. Note that the power throughout a single time step could vary considerably, as it does in the frequency-regulation application. To relate these values to S_t^{E}, the power must be converted into an energy (MWh) by multiplying by the time step t.

The parameters γ_{SD}, γ_{PE} and γ_{B} are the self-discharge, power electronics and battery energy efficiencies, respectively. As our tested systems have no power electronics and low self-discharge rates, it is reasonable for us to assume that both γ_{SD} and γ_{PE} are equal to 1. Here $\gamma_{\mathrm{B}} \leq 1$, which indicates that to supply the grid at an average rate equal to P_t^{D}, the battery must discharge at an average rate of $\gamma_{\mathrm{B}}^{-1}P_t^{\mathrm{D}}$, which is always greater than or equal to P_t^{D}. For all applications, physical constraints on the battery are imposed, so the internal state of charge (SOC) remains within a preset range (20–80% SOC). Note that the CAISO penalizes the resource if energy is promised and not delivered. The 20–80% SOC range is the largest range we could use to ensure that all of the batteries safely completed the entire duty cycles. The amount of charge and discharge in any time period is constrained by the maximum power rating, which determines the maximum and minimum charge and discharge rates (max P^{C}, min P^{C}, max P^{D} and min P^{D}). The economic model was made for a 1 MWh ESS (the power rating can vary) and scales linearly for any sized ESS.

The energy-to-power (E/P) ratio describes the ratio of the available energy of the ESS to the maximum charging power[10]. The higher the E/P ratio, the more complicated or richer the duty cycle. This is because when a profitable cycle is expected, the optimal use of the ESS involves utilizing the maximum amount of discharge or charge possible, bounded by both the power rating and the state of energy. For a higher E/P ratio, the set of possible charge/discharge cycles for each application rises. Thus, the optimization procedures are now to choose from a larger set, hence most often we obtain more charges/discharges and therefore a more complex set of duty cycles. In this article, we develop duty cycles for ESSs with effective E/P ratios of 1 and 3. We then present the results of the performances of several battery chemistries that perform these duty cycles. Batteries have a

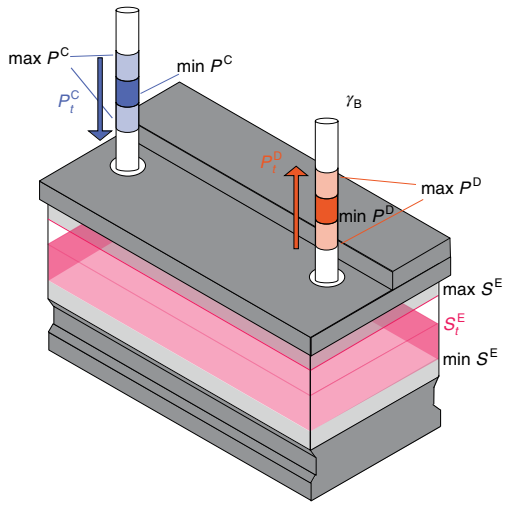

Fig. 2 | The model of a battery used in the economic modelling of the duty cycles. The algorithms developed considered the following parameters: charge rate (max P^C, min P^C and P_t^C), where max P^C and min P^C are the maximum and minimum amounts, respectively, of power that can be taken from the grid by the battery; discharge rate (max P^D, min P^D and P_t^D), where max P^D and min P^D are the maximum and minimum amounts, respectively, of power that can be delivered to the grid by the battery; available energy (max S^E, min S^E and S_t^E), where S_t^E is internal energy of the battery at time t and max S^E and min S^E are the maximum and minimum amounts, respectively, of energy that the battery can store in its operational charge window.

limited amount of energy, and so for our cell-level testing, adjustments to the E/P ratios were realized in adjustments in the power used by the battery. The parameters discussed above are intrinsic to the ESS that are common across all the applications. The application-specific optimizations are explained briefly below and in more detail in Methods.

Revenue and duty cycles

The application duty cycles were primarily designed to maximize the potential revenue of an ESS in one of the products that the CAISO offers. Our approach followed and extended the Electric Power Research Institute methods and tools for the evaluation of electricity storage laid out in the 2013 handbook written by Sandia National Laboratories[11] as well as being tailored towards the California market. The handbook outlines potential grid applications and energy storage technologies that could take advantage of these. The methods involve identifying opportunities, understanding the requirements of the grid, distinguishing between monetizable and incidental benefits, and finally creating energy-storage business cases. The prices used were those for the LA JOLLA 006 node, which is the appropriate node for a study out of the University of California, San Diego. For each application, we chose a representative set of cycles that occur often.

The time-shift application in the DAM works by charging the ESS when the forecasted price of energy is low, and then discharging the ESS when the forecasted price of energy is high[2–4,6,12]. The congestion-relief application is similar to that of the energy time shift. However, the batteries that perform this function serve to free up bottlenecks in electricity transmission and so more charge/discharge events occur[7]. The flexible ramping application accounts for the power fluctuations required to adjust to energy delivery over periods of the order of five minutes[6]. Lastly, the frequency-regulation application is designed to synchronize the supply and demand on the electricity grid[2,12,13]. It is important for the storage system that performs this task to be able to respond quickly to pulsed-power, regulation-up and regulation-down signals. It is important to note that the regulation application assumes that the ESS is operated in the non-REM (Regulation Energy Management for a Non-Generating Resource) mode. This means that the owner of the ESS maintains control over the SOC of the device.

To calculate the revenues and duty cycles for the time-shift application in the DAM, we obtained the price in the form of the locational marginal price, load and forecast load data from the CAISO website for hourly prices over the period from January 2012 until the end of 2014. We used these data to generate forecasts for each hour of each day for the last year of this period using a model for each hour of the day that incorporated past prices (one year) and load data. Forecasts were made at 10:00 the day prior to scheduling the storage device (this is the rule for participating in the California DAM) using only past data. The forecast data were used in conjunction with a linear programming optimization to construct a schedule for each day that maximized the expected revenues based on the forecasted prices, where use of the storage device was constrained by the efficiency and energy of the device as per the described model (Fig. 2) for the battery. This optimization produced actual daily revenues based on the actual prices realized, as well as a duty cycle for the operation of the battery. The locational marginal price consists of the marginal cost of energy, marginal cost of congestion (MCC) and marginal cost of loss components. For the congestion-relief application, we undertook the same steps as for the time-shift application, but schedules were optimized to minimize the congestion at the node as defined by the MCC. This has the effect of charging when congestion is low and discharging when congestion is high.

For the regulation and ramping markets, revenue is gained through offering the service (in the form of capacity payments), as well as energy payments when called upon to provide the service. By the CAISO rules, capacity payments are payments made for providing the opportunity for CAISO to add or remove energy, which are paid for regardless of whether or not energy is provided. Our optimization algorithm used simulated data and capacity payment data. Forecasts were made 75 minutes prior to scheduling the storage device (this is the rule for participating in the California RTM) using only past data. For regulation markets, a single week of state-level demand data was available at the time of the study. Capacity payment data were available for the regulation market, and we constructed forecasts for prices as in the time-shift application. For the ramping market, at the time of the study, no market was in place, so we built a model based on the description by CAISO and used a fixed capacity price of US$5 MW^{-1}. This is the lower end number that the CAISO used in their explanations for how it might work in their Draft Technical Appendix published in June 2015[14]. In these two applications, the ESS owner cannot determine the SOC because it is unknown if the service will be called upon. We ensure that the SOC stays within its limits by tracking the bounds on it (which are known) and periodically charging and/or discharging in the RTM to return the battery to a known SOC.

For the time-shift and congestion applications, the duty cycles produced fluctuated hourly for two years, and for the regulation and ramping applications they fluctuated every 15 minutes for two years. These duty cycles were condensed into schedules for battery testing by choosing a one-week duty cycle representative of the two years of cycling.

Important battery parameters and their relationships

There is a large amount of research on the advantages and drawbacks of a variety of potential electrochemical storage technologies for their use on the grid[10,11,13,15–17]. Five different battery chemistries were used for testing in this article. Lithium ion batteries that contained $LiFePO_4$ (lithium iron phosphate; LFP) and $LiNi_{1/3}Mn_{1/3}Co_{1/3}O_2$ (lithium nickel manganese cobalt oxide; NMC)

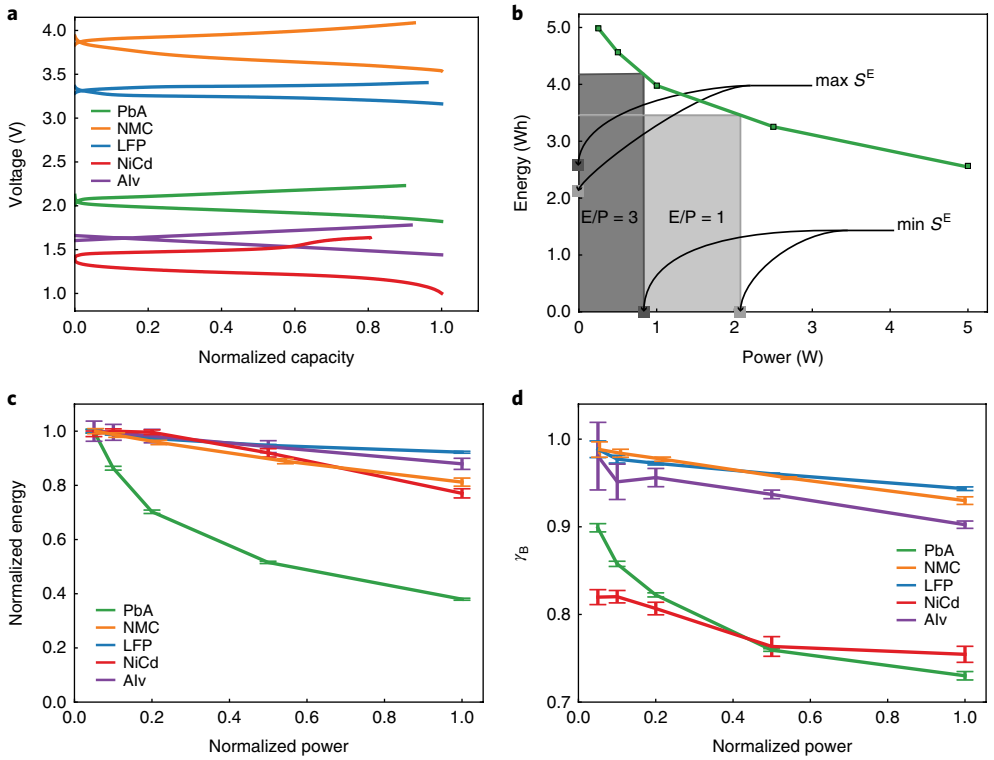

Fig. 3 | Preparatory electrochemical testing and Ragone data. a, Charging/discharging the five batteries at constant power for one hour. Charge and discharge power are the same, so current is higher on discharge than on charge. **b**, An individual Ragone of a PbA battery. The battery was cycled at constant power at rates that correspond to E/P ratios of 20, 10, 5, 2 and 1 according to the rated energy of the battery (from left to right). The green line shows the splined fit of the charge energy of the battery. Light grey squares indicate max P^C and max S^E for E/P = 1, and dark grey squares indicate the same values for E/P = 3. The value of max S^E is equal to the SOC range multiplied by the total available energy at max P^C. **c**, Normalized Ragone data of the five tested battery chemistries. The batteries were cycled at constant power at rates that correspond to E/P ratios of 20, 10, 5, 2 and 1 (from left to right). The curves show the splined fit of the charge energies of the batteries. **d**, Energy efficiency of the five chemistries at rates correspond to the E/P ratios in **c**. The curves show the splined fit. Error bars in **c** and **d** show the standard error of the energy efficiency at each rate with a sample size of ten batteries of each chemistry.

cathodes paired with a graphite anode, as well as nickel cadmium (NiCd) and PbA batteries were purchased from reputable vendors (described in Methods). Finally, 'Alv' refers to aqueous-based sodium ion batteries received from Natron Energy (formerly Alveo Energy[18]). The batteries from Natron Energy were engineering prototypes with significant room for improvement.

Battery manufacturers often only supply a single energy rating for a singular rated current. Although this is a common testing method that is arguably sufficient for common battery applications, to maximize the revenue obtainable on the grid, the relationship between the power output and energy capability needs to be carefully considered (differences in time-limited constant current and constant power cycling are shown in Supplementary Fig. 1). We present a protocol utilizing Ragone plots[19] that allows us to select the optimum charging and discharging power to be used to maximize the revenue obtainable by the storage device. This method enables us to vary the E/P and SOC ratios utilized, and to partially account for the different energy efficiencies of each battery chemistry to maximize the battery's utility. By using this method, we more accurately depict how a battery would be used on the grid and can obtain more accurate efficiency and revenue estimates.

Predicting the efficiency and available energy at an operational power is difficult (Supplementary Fig. 2 shows the result of a significant over-estimation of γ_B). To ensure the safe operation and successful completion of each duty cycle by each of the chemistries, the cells were cycled in a limited SOC window, which, as previously mentioned, we chose as 20–80% of the maximum capacity of each battery charged at max P^C. This window was based primarily on the performance of the PbA and NiCd batteries, whose efficiencies were more difficult to predict. The larger cell-to-cell efficiency variation of the PbA and NiCd batteries when compared to the lithium ion batteries is seen in the larger standard error bars shown in Fig. 3d. This means that in the economic model described above, max S^E actually refers to the energy of the battery that corresponds to the middle 60% of its entire energy capacity range at a given power, max P^C. As there are penalties imposed for being unable to deliver the promised energy on the grid, ESSs on the grid operate in a similar manner.

Applications on the CAISO grid involve dispatches of controlled amounts of power for predetermined periods of time[20]. The effect of charging and discharging at the same constant power for one-hour periods is shown in Fig. 3a for each chemistry. As the voltage is lower during charge than discharge and:

$$P = IV \tag{2}$$

where P is the power, I the current and V the voltage, for equal power the current during discharge is higher than that during charge. This means the battery will run out of capacity if subjected to many of these steps. To maximize the revenue of the battery while operating in a safe SOC range, we set:

$$\max\ P^D = \gamma_B \max\ P^C \tag{3}$$

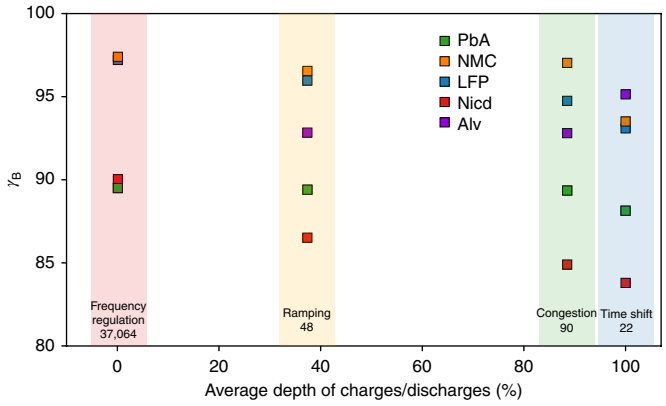

Fig. 4 | Energy efficiencies of batteries performing the application-based duty cycles. E/P = 1 duty cycles are characterized by the average depth of charges/discharges and by the number of charge/discharge events per week. The numbers below the labels show the number of charge/discharge events per week. The average energy efficiencies from the week-long duty cycles are shown for each battery chemistry. At the time of testing the Natron Energy battery, the frequency-regulation duty cycle had not been finalized and so the efficiency result is not included.

To select the optimal value of max P^C to be used by the battery in each application, we utilized our Ragone diagrams of each chemistry. These diagrams also allowed us to estimate the value of γ_B for each chemistry in each application. An individual Ragone diagram of a PbA battery is shown in Fig. 3b. The battery was cycled at rates that correspond to E/P ratios of 20, 10, 5, 2 and 1 (from left to right) according to the rated energy of the battery. To obtain the correct max P^C and max S^E to use for the applications, the SOC range needed to be considered. We used the gradient of the splined Ragone diagram to solve equation (4) to find the optimum energy and power values:

$$\max P^C = \frac{(\mathrm{SOC}_{\mathrm{lim}}^{\max} - \mathrm{SOC}_{\mathrm{lim}}^{\min}) E_T}{\mathrm{E/P\ ratio}} \quad (4)$$

Here, E_T refers to the total available energy of the battery should the entire SOC be used, $\mathrm{SOC}_{\mathrm{lim}}^{\max}$ is the upper SOC limit (as a proportion of the available E_T,which was set to 0.8 here), $\mathrm{SOC}_{\mathrm{lim}}^{\min}$ corresponds to the lower SOC limit and was set to 0.2. The operational energy, max S^E, and maximum power, max P^C, used for E/P = 1, are shown in Fig. 3b. Equation (5) gives max S^E:

$$\max S^E = E_T (\mathrm{SOC}_{\mathrm{lim}}^{\max} - \mathrm{SOC}_{\mathrm{lim}}^{\max}) \quad (5)$$

Once max S^E and max P^C are found, γ_B is estimated by interpolating the voltaic efficiency of the battery at max P^C.

Fig. 3c and Fig. 3d show how the available energy and efficiency of each of the chemistries vary with power. The batteries were cycled at rates corresponding to E/P ratios of 20, 10, 5, 2 and 1 (from left to right) according to the rated energy of the battery. As well as providing us with a method to accurately replicate how a battery would be used on the grid, these Ragone diagrams give us an indication of characteristics of the chemistries that might be important for different applications. For example, although NiCd had generally poor efficiency (Fig. 3d), it maintained good rate performance (Fig. 3c) when compared with PbA.

Relationships between duty cycles and battery chemistries

Once the parameters for each application and chemistry were calculated, the batteries were tested on the duty cycles. The time-shift and congestion applications involve periods of deep charge/discharge[2,3,10,21], whereas the ramping and frequency-regulation cycles are power-based applications and move smaller amounts of energy with each charge and discharge[2,13,22]. Supplementary Figs. 8–17 show the power profiles and the corresponding SOC of the battery chemistries. The duty cycles include an additional 'top-off' step (Supplementary Fig. 2), which allows us to extract from the efficiency its coulombic and voltaic components. The efficiency of each battery is calculated for each day of each duty cycle. Interesting interday variations occur due to the nature of the studied applications (Supplementary Figs. 4,5,6 and 7 and Supplementary Note 1). In Fig. 4, we show the average week-long efficiencies of each of the battery chemistries that undergo the different applications at E/P = 1.

It is known that the efficiency of a battery varies greatly with its chemistry[10,15,20,23,24]. For all the duty cycles, the lithium ion chemistries (NMC and LFP) had the highest efficiencies of the commercial batteries tested, whereas the NiCd chemistry had the lowest efficiency. The efficiency of the sodium-ion batteries (Alv) were impressive, yet inconsistent. These batteries were under development at the time, which probably led to the large interbattery variance. The results for E/P = 3, shown in Supplementary Fig. 3, follow a similar trend.

Evaluating the performances of the chemistries undergoing the duty cycles yields two key insights. First, the duty cycles have substantially different effects on the efficiencies of the batteries. For all the commercial batteries, the efficiency during the time-shift application was always the lowest and was always highest for the frequency-regulation application. Second, the magnitude of the influence of the duty cycles on the efficiencies varies with each chemistry. In moving from the time-shift to frequency-regulation duty cycles, the energy efficiency, γ_B, of the NiCd chemistry changes from 83.8 to 90.3%, a difference of 6.5%. For the PbA chemistry, γ_B changes only from 88.1 to 90.0%, a difference of 1.9%. This mismatch in efficiency between chemistries and duty cycles becomes important in evaluating the use of a particular chemistry in different grid-scale applications, as is shown when combined with the revenue results.

Influence of battery efficiency on revenue

The results in Fig. 5 show how revenues improve as the energy efficiency, γ_B, improves. For applications that require deep discharge (time shift and congestion) improvements arise, as for each opportunity to generate revenue, a larger amount of energy can be discharged to, or taken from, the grid. The linear increases in revenue follow as increases in efficiency simply increase the payment for each cycle. For regulation and ramping, the majority of revenue arises from capacity payments. The increasing slopes of the effect of efficiency on revenues arise as the greater available energy allows the storage to offer proportionally greater energy over time.

To establish a more real-world evaluation of the value of different chemistries in different applications, Table 1 reports the average efficiencies and revenues at those efficiencies where the efficiencies are found from the batteries that perform the appropriate duty cycles at E/P = 1. Examining revenues based on experimental efficiencies allows a greater insight into the relationships between the chemistry choices and the applications of the batteries. First, revenue calculations at full efficiencies are misleading, not only in the size of the revenue, but also they indicate that the best application of the battery is for applications like time shift or ramping. The results show that at 100% efficiency there is a statistically significantly higher revenue for time shift than for regulation. However, for high-efficiency chemistries, such as those based on the lithium ion (LFP and NMC), more revenue is generated in regulation than in time shift because of the differences in efficiencies across the applications. The second implication that arises is that there can be a strong variation

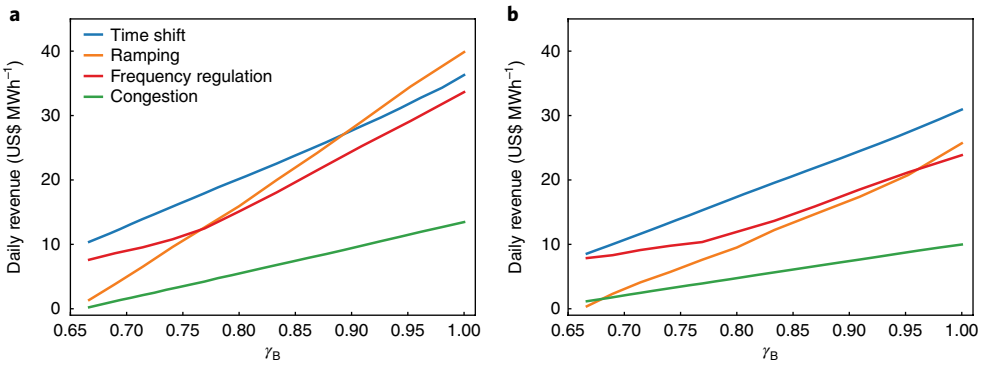

Fig. 5 | The revenue versus the efficiency for the different application duty cycles. a, E/P = 1. **b**, E/P = 3.

Table 1 | Average efficiencies and corresponding revenues for each duty cycle and chemistry combination for batteries undergoing the duty cycles at E/P = 1

Duty cycle	Revenue	Battery chemistry					
		100%	PbA	LFP	NiCd	NMC	Alv
Time shift	Efficiency (%)	100.0	88.1	93.1	83.8	93.5	95.1
	Revenue (US$)	36.3	26.2	30.1	22.9	30.5	31.8
Congestion	Efficiency (%)	100.0	89.4	94.8	84.9	97.0	92.8
	Revenue (US$)	13.5	9.1	11.4	7.4	12.3	10.6
Ramping	Efficiency (%)	100.0	89.4	96.0	86.5	96.6	92.8
	Revenue (US$)	39.9	27.1	35.7	23.8	36.5	31.8
Regulation	Efficiency (%)	100.0	89.9	97.2	90.0	97.4	N/A
	Revenue (US$)	33.6	24.3	31.1	24.4	31.2	N/A

of efficiencies across applications that shift the relative value of any application to each technology. For all the chemistries, efficiency is higher for the duty cycles that require lower fluctuations in the SOC, like regulation. However, the relative gains in efficiency (across duty cycles) differ across chemistries, being small for PbA and larger for the other chemistries. This has the result that for most of the chemistries, regulation improves revenue relative to time shift, which is not true for PbA. Finally, for a low revenue application, such as congestion relief, differences in efficiencies are far less important because the revenue is relatively flat over the efficiency of the battery, so lower-efficiency chemistries are relatively more valuable in these applications over the high-efficiency chemistries.

Conclusion

There is substantial variation in the potential revenue generation reported in the literature. By making modelling choices that replicate real-world applications as closely as possible and, when it is available, by using large amounts of data to construct our models, we have provided a reliable understanding of the potential revenues obtainable by an ESS on the California grid. We also developed a technique for accurately measuring the performance of cell-level battery chemistries undergoing duty cycles representative of these applications. This technique demonstrates the importance of understanding the efficiencies and rate performances of batteries subject to use.

More importantly, contrary to the current literature, we show that to accurately gauge the potential revenue of an energy storage technology on the grid, it is insufficient to assume constant efficiencies across different applications. As an example, for the LFP battery, if one were to assume that the efficiency of the time-shift application (93.1%) was consistent across all of the battery applications, this would result in a substantial error in the calculations of revenue. For congestion, ramping and frequency-regulation applications, the percentage error in calculated revenue would be 6, 11 and 15% respectively. The combined results of our economic modelling and cell-level testing demonstrate that different grid-scale applications affect the energy efficiencies of different battery chemistries in different ways. These effects alter the relative value of each battery chemistry in each application, which potentially result in a change in the optimal chemistry–application pairings. To gain further insight into the different effects that application duty cycles have on ESSs, a larger variety of battery chemistries and energy storage technologies (including larger scale and more complete storage systems) will be tested. Longer-term testing will be completed to observe the effects of different application duty cycles on the lifetime performance of the different energy storage technologies. Finally, additional duty cycles will be created by exploring other applications as well as stacking multiple applications together.

Combining the effects of efficiency, lifetime performance and cost analyses of storage technologies with respect to each grid-scale application will provide a more nuanced understanding of the relative benefits of different technologies to be used to for grid-scale storage. This study illustrates the importance of considering the relationships between applications, chemistries and efficiencies to obtain the potential revenues of ESS on the grid and could result in a paradigm shift in the way that energy storage technologies are evaluated for grid-scale use.

Methods

Revenue and duty-cycle development. The CAISO provides public market results data via the Open Access Same-Time Information System web portal[25]. The primary node of interest is LAJOLLA_6_N001 at which energy imports/

exports between University of California San Diego and CAISO are settled. LAJOLLA_6_N001 is located south of transmission paths 15 and 26, and hence we mapped it into ancillary service regions AS_CAISO, AS_SP15 and AS_SP26 and their expanded forms. The four application duty cycles were developed to maximize revenue in four products that the CAISO offers: energy time shift, congestion relief, frequency regulation and flexible ramping. All of the decisions by the algorithm were made in 'real time' using only data that would be available to an operator in the construction of forecasts on which decisions are based. To start in January 2013 and use past data we required data before January 2013 to construct the forecasts. This is why we obtained 3 yr of data, where available, from January 2012.

Time-shift and congestion revenues. For the time-shift application, we used the DAM data and obtained hourly price and load data from January 2012 to December 2014. As with all price data (DAM and RTM), the price data are made up of three components. The locational marginal price (US$ MWh^{-1}) consists of the marginal cost of energy, MCC and marginal cost of loss components. We downloaded hourly locational marginal prices and their energy, congestion and loss components (US$ MWh^{-1}). We made forecasts of the price and load from January 2013 to December 2014. The forecasting model considered past prices and load data. Forecasts for each day were made and locked in at 10:00 the prior day as per the CAISO rules. Using these forecasted prices and loads and the physical limits and characteristics of the battery (Fig. 2), a linear optimization program constructed the schedules for each day. These schedules were applied to the actual load and pricing data to give accurate revenue results. The algorithm also produced a 2 yr long duty cycle for the application. From the 2 yr long duty cycle, a representative week-long duty cycle was created. For the congestion application, the methods were almost identical to that of the time-shift application; however, this application was optimized to minimize the expected congestion component. This means that the battery charges when the MCC is low, and discharges when the MCC is high.

Ramping revenue. At the time of the study there was no market in place for the ramping application. To model the demand and energy prices we constructed a model based on the description by the CAISO[14]. The flexible ramping requirement is made up of two components, the part due to the net demand forecast change and that due to uncertainty over this net demand forecast. The CAISO attempts to find a percentile of the forecast distribution of energy supplied, constructed as a mean plus forecast error variation around the mean. These numbers are constructed by using the running of the market clearing algorithm at the time energy is committed (which has a forecast of demand change) and the value determined right before delivery. For our models, we use an approximation to determine, for any 15 min interval, whether or not the ramping up or ramping down markets will be operational. The reason we do not need the overall quantity of demand in these markets is that the storage devices we consider are very small relative to the overall markets, and hence we assume that the quantity demanded will be far in excess of the capacity of the storage device.

To do this in the absence of the results from the real-time algorithm that clears the market prices, we approximated the process using the 5 min load data available from the CAISO. These data are for all of California. We used these data to construct forecasts of the 5 min load using rolling forecasts. These forecasts were then used with the load data to construct whether or not demand for flexible ramping up or down is likely for any 5 min interval. However, bidding in the RTM is done on a 15 min basis. We aggregated to 15 min periods by assuming that if the market is operational for any 5 min period in the 15 min, then it is operational. For our revenue calculations, this means that if we have an energy bid in the RTM for a particular 15 min period and we have the capacity to offer ramping (typically, this means that if we are buying energy at full power, we allow the CAISO to reduce power and hence allow ramping down and then obtain less power than we contracted for, the opposite to that when we have a bid that is selling energy to the grid), then we can offer it so long as the market is operational. If not, we cannot make a bid in this market. We used a fixed capacity price of US$5 MW^{-1}.

In the CAISO rules, there is no guarantee of the actual uptake of energy once a bid is confirmed. This means that the battery owner loses control of the SOC and must recharge it in the RTM. Due to the CAISO rules, this requires waiting 75 min after each use of the battery in the regulation market. The linear optimization program takes this stipulation and the forecasted prices of the RTM into consideration when producing the optimal schedule for operating in the regulation market.

Frequency-regulation revenue. For the frequency-regulation application, the capacity payment and mileage payment data were available from January 2012 to December 2014. Demand and pricing forecasts were constructed in a similar method to that of the time-shift and congestion cycles. The demand data for the frequency-regulation application were simulated. The CAISO only provides a single week of state level demand data in the form of an Automatic Generation Control (AGC) signal. The AGC signal provides the system-wide capacity procured every 4 s, giving 151,200 intervals. The data include values for the regulation down capacity, regulation up capacity and the AGC signal for procurement. The first two of these are positive, and the AGC signal follows the CAISO convention of being positive for energy supplied by generation (regulation up) and negative for energy removed by generation (regulation down). We aggregated these data to the payment period and constructed probabilities of up or down regulation demand based on the aggregate data (this is relevant because payments are also on the aggregate).

There are instances for which the AGC signal capacity is higher than the system-wide capacity indicated. For these, we set the AGC signal equal to capacity (this is 'AGC trimmed' in the data). For any 4 s interval (observation) we computed the proportional take-up of capacity in any period while preserving the sign that indicates regulation up or down. As discussed in the previous section on ramping, the application of the battery in this market (non-REM regulation) results in no guarantee of uptake of the offer for regulation services. We followed a similar strategy to that on ramping to ensure the battery did not exceed its SOC limits. Downtime waiting for charge/discharge in the RTM reduces the value of the battery in this application.

To model week-to-week variation through the 2 yr, we followed an approach in Donadee and Wang that models the demand using an AGC signal at the hourly level relevant for cost calculations[26]. In this model, demand for regulation up and regulation down is modelled as a function of the previous hour demand and a function of the AGC signal plus four variables that capture intraday seasonality using a Fourier approximation. We ran the regression for the week of data from the CAISO to estimate the coefficients of the model separately for regulation up and regulation down and estimated the residuals from these regressions. The 2 yr long demand sequence was then generated from these regressions (again separately for regulation up and down) using a non-parametric bootstrap.

Cell-level testing. Tests were carried out on the batteries using an Arbin Laboratory Battery Testing cycler. Each duty cycle was carried out on a separate battery. The lithium ion (LFP and NMC) and NiCd batteries were purchased from Tenergy[27–29]. The PbA battery was purchased from EnerSys[30]. The Alv battery was provided by Natron Energy (formerly Alveo Energy[18]) and was under development at the time. Due to the availability of the batteries from Tenergy, the LFP and NiCd batteries were tested using two different form factors. These batteries differed only in the capacity of the battery. Using the Ragone method to calculate the correct max S^E and max P^C for each application ensured that the different sizes of the batteries had no impact on the efficiency calculations.

Ragone. Prior to each Ragone test, each battery underwent three break-in cycles, cycling at constant power at rates equivalent to E/P = 2 according to the manufacturers' advertised cell capacity between the manufacturer's specified voltage limits. A power cycle at a rate equivalent to E/P = 20 was then performed before carrying out the Ragone test. The Ragone test was executed by power cycling the battery at rates equivalent to E/P ratios of 20, 10, 5, 2, 1. The Ragone data shown in Fig. 3c,d is averaged over ten results for each battery chemistry.

As described in Fig. 3, the estimations of max S^E and max P^C were made from the Ragone plot for each battery and each application for E/P ratios of 1 and 3. Subsequently, an estimation of γ_B was interpolated from the voltaic efficiency versus power plot. Originally, we had used the energy efficiency at each power (Fig. 3b), but this often resulted in an underestimation of the efficiency, and so we switched to using the voltaic efficiency. For the time-shift, congestion and frequency-regulation applications, the SOC limit (20–80%) was selected to ensure that all the battery chemistries could safely, and repeatedly, complete the week-long duty cycles. This limit was primarily based on the performance of the PbA and NiCd batteries, whose voltaic efficiencies were difficult to estimate. Supplementary Fig. 2a shows the result of a significantly incorrect estimation of γ_B for a NiCd battery. Due to the overestimation of the efficiency, the battery rapidly approaches and surpasses its voltage limits, which causes failure. Although extending the SOC limits allows a larger portion of the battery to be used, it ultimately leaves less room for error.

Time-shift and congestion testing. Prior to each duty cycle, the batteries were power cycled at the selected operational power for each duty cycle (max P^C and max P^D). The maximum charge capacity of this cycle was used to calculate the SOC for the rest of the duty cycle. The power profiles of each duty cycle and the corresponding SOC of the different battery chemistries are shown in Supplementary Figs. 8a–17a (time shift) and 8b–17b. (congestion). At the end of each day, a top-off step was performed (Supplementary Fig. 1b). The batteries were discharged at power max P^D to their advertised lower voltage limit, and then recharged at power max P^C to the correct SOC to begin each day. For the time-shift and congestion applications, the economic results set this to 20% of the entire SOC range. In the literature, batteries are often charged and discharged to SOC limits based on capacity[7]. This artificially sets the coulombic efficiency to 100%. By adding this top-off step we are able to separate the energetic efficiency into its coulombic and voltaic components. This separation helps us to better understand the effects of the duty cycles on the chemistries (Supplementary Figs. 6 and 7).

Ramping testing. As there were no available data provided by the CAISO on the shape of the ramping cycle, a linear ramp from 0 W to max P^C and max P^D, was used for each event of the duty cycle. This meant that in each step of the duty cycle, the average (operational) power was equal to max $P^C/2$. This operational power was used for the initial cycle and the top-off steps during the ramping cycle. This had the effect of altering the operational SOC range of the ramping duty cycles to between 40 and 60% of maximum capacity. The top-off steps brought the SOC to 50% at the start of each day. This beginning SOC was dictated by the shape of the application duty cycles where there is a possibility that either ramping up or down could generate the most revenue. We chose to test the ramping duty cycles in this manner to respect the power limits imposed by the battery and the E/P ratio. The power profiles of each duty cycle and the corresponding SOC of the different battery chemistries are shown in Supplementary Figs. 8c–17c.

Frequency-regulation testing. The CAISO only provides a week-long snap-shot of the power profile of the frequency-regulation signal. This is in the form of an AGC signal with fluctuations in power every 4 s, which gives 15,200 intervals, and the regulation up and down capacity demand profiles that fluctuate every 15 min. To simulate the action of an ESS performing this application, we used the information provided by the economic simulation on when it would be most profitable for an ESS to participate. This information was provided in the form of a duty cycle that fluctuates on a 15 min basis where the ESS is either participating, resting or charge balancing (returning to 50% of its SOC). As an example, a 2 h snap shot of the duty cycle for an E/P = 1 ESS is shown as $[A_1,A_2,0,0,0,0,B_1,B_2]$, where A denotes that the ESS is participating in the frequency-regulation application, 0 denotes that the ESS is resting and B denotes the ESS is charge balancing. The subscripts indicate application/charge-balancing pairs. The CAISO rules dictate that the ESS owner must wait 75 min before charging/discharging in the RTM after a successful bid. As the energy uptake of participating in the application is unknown prior to the completion of the application and the ESS is limited by maximum power bounds, if an ESS participates in the application for 15 min, a 15 min period must be allotted to ensure with certainty that the SOC of the ESS is restored. By the above CAISO rule, this charge-balancing period must be at least 75 min after the application period. If E/P = 1, the maximum number of consecutive periods that the battery can participate in the frequency-regulation application is two. The battery begins each period at 50% SOC. There is potential for the application to demand full power for the whole period, which would use 25% of the available energy. Therefore, to ensure certainty of operation, an ESS with an E/P ratio of one can only participate in two consecutive periods of the application when its full power capacity is bid. Similarly, if E/P = 3, the maximum number of consecutive periods that the battery can participate in the frequency-regulation application is six. This has the interesting effect that the battery does not have to undergo a rest state as it can participate in the frequency-regulation application during the 75 min waiting period required before charge balancing. A 3 h snap shot of the duty cycle for an E/P = 3 ESS is shown as $[A_1,A_2, A_3,A_4,A_5,A_6,B_1,B_2, B_3,B_4,B_5,B_6]$. The power profiles of each duty cycle and the corresponding SOC of the different battery chemistries are shown in Supplementary Figs. 8d–15d.

After the duty cycles were finalized, each battery chemistry was tested at least twice for each application at E/P ratios of 1 and 3. The efficiency data showed good reproducibility both in the values of the efficiencies and in the interday efficiency trends that arise from the different power profiles on each day. The efficiency data presented in the paper are averaged from the number of batteries tested on each application at each E/P ratio (Fig. 4 and Supplementary Figs. 3–5).

Data availability

The data that support the plots and tables within this article, and the other findings of this study, are available from the corresponding authors upon reasonable request. Additionally, open source access to the duty cycles produced in this article is available at http://econweb.ucsd.edu/~gelliott/Charges.html.

Received: 27 July 2017; Accepted: 24 October 2018;
Published online: 03 December 2018

References

1. Eyer, J. & Corey, G. *Energy Storage for the Electricity Grid: Benefits and Market Potential Assessment Guide. A Study for the DOE Energy Storage Systems Program* (Sandia National Laboratories, 2010).
2. Walawalkar, R., Apt, J. & Mancini, R. Economics of electric energy storage for energy arbitrage and regulation in New York. *Energy Policy* **35**, 2558–2568 (2007).
3. Sioshansi, R., Denholm, P., Jenkin, T. & Weiss, J. Estimating the value of electricity storage in PJM: arbitrage and some welfare effects. *Energy Econ.* **31**, 269–277 (2009).
4. Figueiredo, F. C., Flynn, P. C. & Cabral, E. A. The economics of energy storage in 14 deregulated power markets. *Energy Stud. Rev.* **14**, 131–152 (2006).
5. Byrne, R. H., Concepcion, R. J. & Silva-Monroy, C. A. Estimating potential revenue from electrical energy storage in PJM. In *2016 IEEE Power and Energy Society General Meeting (PESGM)* (IEEE, 2016); https://doi.org/10.1109/PESGM.2016.7741915
6. Fitzgerald, G., Mandel, J., Morris, J. & Touati, H. *The Economics of Battery Energy Storage: How Multi-Use, Customer-Sited Batteries Deliver the Most Services and Value to Customers and the Grid* (Rocky Mountain Institute, 2015).
7. Conover, D. et al. *Protocol for Uniformly Measuring and Expressing the Performance of Energy Storage Systems* (Pacific Northwest National Laboratory, Sandia National Laboratories, 2016).
8. Linden, D. & Reddy, T. *Handbook of Batteries* 4th edn (McGraw-Hill, New York, 2010).
9. Kjaer, S. B., Pedersen, J. K. & Blaabjerg, F. A Review of single-phase grid-connected inverters for photovoltaic modules. *IEEE Trans. Ind. Appl.* **41**, 1292–1306 (2005).
10. Leadbetter, J. & Swan, L. G. Selection of battery technology to support grid-integrated renewable electricity. *J. Power Sources* **216**, 376–386 (2012).
11. Akhil, A. A. et al. *DOE/EPRI Electricity Storage Handbook in Collaboration with NRECA* (Sandia National Laboratories, 2015).
12. Byrne, R. H., Donnelly, M. K., Loose, V. W. & Trudnowski, D. J. *Methodology to Determine the Technical Performance and Value Proposition for Grid-Scale Energy Storage Systems* (Sandia National Laboratories, 2012).
13. Xu, B., Dvorkin, Y., Kirschen, D. S., Silva-Monroy, C. A. & Watson, J.-P. A Comparison of policies on the participation of storage in U.S. frequency regulation markets. In *2016 IEEE Power and Energy Society General Meeting (PESGM)* (IEEE, 2016); https://doi.org/10.1109/PESGM.2016.7741531
14. California Independent System Operator Corporation *Flexible Ramping Product: Revised Draft Final Proposal* (CAISO, 2015).
15. Dunn, B., Kamath, H. & Tarascon, J.-M. Electrical energy storage for the grid: a battery of choices. *Science* **334**, 928–935 (2011).
16. Yang, Z. et al. Electrochemical energy storage for green grid. *Chem. Rev.* **111**, 3577–3613 (2011).
17. Akhil, A., Zaininger, H., Hurtwitch, J. & Badin, J. *Battery Energy Storage: A Preliminary Assessment of National Benefits (The Gateway Benefits Study)* (Sandia National Laboratories, 1993).
18. Natron Energy announces technology evaluation agreement with EDF for grid storage applications. *BusinessWire* (10 July 2018).
19. Ragone, D. V. *Review of Battery Systems for Electrically Powered Vehicles*. SAE Technical Paper 680453 (SAE, 1968); https://doi.org/10.4271/680453
20. Joseph, A. & Shahidehpour, M. Battery storage systems in electric power systems. In *2006 IEEE Power Engineering Society General Meeting* (IEEE, 2006); https://doi.org/10.1109/PES.2006.1709235
21. Byrne, R. H. & Silva-Monroy, A. *Estimating the Maximum Potential Revenue for Grid Connected Electricity Storage: Arbitrage and Regulation* (Sandia National Laboratories, 2012).
22. Nguyen, T. A., Byrne, R. H., Concepcion, R. J. & Gyuk, I. Maximizing revenue from electrical energy storage in MISO energy frequency regulation markets. In 2017 *IEEE Power & Energy Society General Meeting* (IEEE, 2017); https://doi.org/10.1109/PESGM.2017.8274348
23. Luo, X., Wang, J., Dooner, M. & Clarke, J. Overview of current development in electrical energy storage technologies and the application potential in power system operation. *Appl. Energy* **137**, 511–536 (2015).
24. Divya, K. C. & Østergaard, J. Battery energy storage technology for power systems—an overview. *Electr. Power Syst. Res.* **79**, 511–520 (2009).
25. California ISO (OASIS, accessed 23 May 2017); http://oasis.caiso.com/
26. Donadee, J. & Wang, J. AGC signal modeling for energy storage operations. *IEEE Trans. Power Syst.* **29**, 2567–2568 (2014).
27. *Specification Approval Sheet—LiFePO$_4$ Rechargeable Battery* (Tenergy, 2014); http://www.all-battery.com/datasheet/30067_datasheet.pdf
28. *Specification Approval Sheet—Lithium-Ion Rechargeable Battery* (Tenergy, 2010); http://www.tenergy.com/30001_datasheet.pdf
29. *Specification Approval Sheet—Nickel Cadmium Cylindrical Cell* (Tenergy, 2012); http://www.tenergy.com/20203_datasheet.pdf
30. *Cyclon Batteries* (EnerSys, 2008); http://www.enersys.com/Cyclon_Batteries.aspx?langType=1033

Acknowledgements

This work was supported by the Advanced Research Projects Agency–Energy (ARPA-E), the US Department of Energy under award no. DE-AR000520 as part of the Cycling Hardware to Analyze and Ready Grid-Scale Electricity Storage (CHARGES) program. The authors express their gratitude to B. Torre and A. Tong for their time and valuable discussions, especially with regards to the applicability of this study to larger-scale ESSs. The authors also thank T. Wynn, C. Rustomji and P. Parikh for their help in editing the manuscript.

Author contributions

D.M.D., M.G.V., G.E. and Y.S.M. designed the study. O.M., Y.R.C. and G.E. developed the forecasting techniques and algorithms for the revenue calculations. All authors contributed to developing the duty cycles for the applications. D.M.D., M.G.V. and Y.S.M. developed the cell-level testing protocols. D.M.D., M.G.V. and R.R. performed the cell-level testing and D.M.D., M.G.V. and Y.S.M performed the subsequent data analysis. D.M.D., G.E. and Y.S.M. led the writing of the paper.

Competing Interests

The authors declare no competing interests.

Additional information

Supplementary information is available for this paper at https://doi.org/10.1038/s41560-018-0290-1.

Reprints and permissions information is available at www.nature.com/reprints.

Correspondence and requests for materials should be addressed to Y.S.M. or G.E.

Publisher's note: Springer Nature remains neutral with regard to jurisdictional claims in published maps and institutional affiliations.